Mon. Not. R. Astron. Soc. **000**, 000–000 (0000) Printed 1 February 2008 (MN LATEX style file v2.2)

The high mass end of the Tully-Fisher relation

E. Noordermeer,[1,2⋆] and M. A. W. Verheijen[2]
[1] *University of Nottingham, School of Physics and Astronomy, University Park, NG7 2RD Nottingham, UK*
[2] *Kapteyn Astronomical Institute, University of Groningen, PO Box 800, 9700 AV Groningen, The Netherlands*

accepted version, 20-08-2007

ABSTRACT

We study the location of massive disk galaxies on the Tully-Fisher relation. Using a combination of K-band photometry and high-quality rotation curves, we show that in traditional formulations of the TF relation (using the width of the global HI profile or the maximum rotation velocity), galaxies with rotation velocities larger than $200\,\mathrm{km\,s^{-1}}$ lie systematically to the right of the relation defined by less massive systems, causing a characteristic 'kink' in the relations. Massive, early-type disk galaxies in particular have a large offset, up to 1.5 magnitudes, from the main relation defined by less massive and later-type spirals.

The presence of a change in slope at the high-mass end of the Tully-Fisher relation has important consequences for the use of the Tully-Fisher relation as a tool for estimating distances to galaxies or for probing galaxy evolution. In particular, the luminosity evolution of massive galaxies since $z \approx 1$ may have been significantly larger than estimated in several recent studies.

We also show that many of the galaxies with the largest offsets have declining rotation curves and that the change in slope largely disappears when we use the asymptotic rotation velocity as kinematic parameter. The remaining deviations from linearity can be removed when we simultaneously use the total baryonic mass (stars + gas) instead of the optical or near-infrared luminosity. Our results strengthen the view that the Tully-Fisher relation fundamentally links the mass of dark matter haloes with the total baryonic mass embedded in them.

Key words: galaxies: spiral – galaxies: elliptical and lenticular, cD – galaxies: fundamental parameters – galaxies: kinematics and dynamics – galaxies: statistics

1 INTRODUCTION

The notion of a tight correlation between absolute luminosities of spiral galaxies and their rotational velocities has been with us for about thirty years now (Tully & Fisher 1977). This 'Tully-Fisher' (TF) relation has been confirmed to hold over many decades in luminosity (Courteau 1997; McGaugh et al. 2000; Verheijen 2001) and in different galaxy environments (Giovanelli et al. 1997; Willick 1999). Barred and unbarred galaxies share the same TF relation as well (Courteau et al. 2003), as do high and low surface brightness galaxies (Sprayberry et al. 1995; Zwaan et al. 1995). Although spirals of different morphological types do follow different TF relations (Roberts 1978; Rubin et al. 1985; Hinz et al. 2001; Mathieu et al. 2002; Russell 2004), these offsets disappear almost entirely when using near-infrared photometry, rather than optical luminosities (Aaronson & Mould 1983; Peletier & Willner 1993), indicating that most of the differences at bluer wavelengths can be attributed to variations in star formation history along the Hubble sequence and the resulting differences in stellar populations. Similarly, when dynamical models are used to derive circular velocities for elliptical galaxies, it is found that the latter follow a similar TF relation to spirals, but offset to lower luminosities. This offset can again be explained from differences in the stellar mass-to-light ratios (Gerhard et al. 2001; de Rijcke et al. 2007).

The Tully-Fisher relation has become one of the most widely used relations in extragalactic astronomy. It has been commonly used as a powerful tool to estimate distances to galaxies (e.g. Tully & Pierce 2000, and references therein). As a statistical correlation between fundamental properties of spiral galaxies, it has also been used to constrain numerical simulations of galaxy formation (Dalcanton et al. 1997; Navarro & Steinmetz 2000; Bullock et al. 2001; Pizagno et al. 2006; Portinari & Sommer-Larsen 2007), probe galaxy evolution on cosmological timescales (Vogt et al. 1997; Ziegler et al. 2002; Milvang-Jensen et al. 2003; Böhm et al. 2004; Bamford et al. 2006; Weiner et al. 2006; Chiu et al. 2007), or study the structure and stellar

⋆ email:edo.noordermeer@nottingham.ac.uk

populations of nearby galaxies (Franx & de Zeeuw 1992; Courteau & Rix 1999; Bell & de Jong 2001).

Traditionally, the Tully-Fisher relation was studied using the width W of a galaxy's global neutral hydrogen line profile as a probe for its rotational velocity (Tully & Fisher 1977). With larger samples of spatially resolved kinematics (rotation curves) becoming available, the rotation velocities can be directly measured and recent studies tend to use the maximum rotation velocity ($V_{\rm max}$) instead. This subtle shift has the added advantage that the TF relation can be measured at cosmological distances, using optical spectroscopic observations of high-redshift galaxies (see references above).

Most spiral galaxies have flat rotation curves and for these systems, both kinematic measurements (W and $V_{\rm max}$) generally yield nearly equivalent velocities. However, this is not the case for all galaxies. In galaxies whose rotation curves are rising or declining at large radii, it is not clear a priori which kinematic parameter yields the best results. Verheijen (2001, hereafter V01) presented an extensive study, based on a sample of 31 galaxies in the Ursa-Major cluster with well-defined rotation curves and K-band photometry, of the influence of the shape of a rotation curve on the location of a galaxy on the Tully-Fisher relation. Galaxies with declining rotation curves were found to lie systematically on the high-velocity side, when using the maximum rotation velocity $V_{\rm max}$ or the width of the HI profile. Since these are typically bright systems with high rotation velocities, this result suggests that there may be a change in slope in the TF relation at the high-luminosity end, a possibility also hinted at by Peletier & Willner (1993). Clearly, the existence of a 'kink' in the Tully-Fisher relation has important consequences and, if not corrected for, will lead to systematic biases when deriving cosmological distances or probing galaxy evolution.

However, V01 also showed that the systematic offset at the high mass end disappeared when, instead of $V_{\rm max}$, the asymptotic rotation velocity $V_{\rm asymp}$ in the outer, flat parts of the rotation curve was used. Bearing in mind that the asymptotic rotation velocities are determined by the dark matter haloes, V01 interpreted this result as a strong indication that the TF relation fundamentally links the total baryonic content of (disk) galaxies with their dark matter haloes, and that as far as this relation is concerned, there is no fundamental difference between low and high mass galaxies.

Unfortunately, the sample of V01 only contained a small number of galaxies with declining rotation curves and the declines were modest. Thus, the change in slope of the high-luminosity end of the TF relation when going from $V_{\rm max}$ to $V_{\rm asymp}$ was small and his results only gave a first indication for how to interpret the curvature at the high-mass end of the TF relation in terms of the kinematics of the galaxies. Recently, however, a sample of high-quality rotation curves for high-luminosity early-type disk galaxies (S0 – Sab) has become available (Noordermeer et al. 2007, hereafter N07). This sample contains many strongly declining rotation curves where the difference between the maximum and asymptotic rotation velocities is much larger than in Verheijen's galaxies. In this paper therefore, we combine Noordermeer's sample with the data for the galaxies with flat and declining rotation curves from V01, with the aim of further investigating the change in slope at the bright end of the TF relation and its relation with the shapes of rotation curves. We also include the recent sample of rotation curves from Spekkens & Giovanelli (2006, hereafter S06) in our analysis; these are all massive late-type spiral galaxies with flat rotation curves and provide a valuable benchmark at the high-luminosity end of the TF relation.

The outline of the remainder of this paper is as follows. In section 2, we describe the selection of galaxies from the three different samples for the present study, together with the photometric and kinematic ingredients for the TF analysis. In section 3, we present the Tully-Fisher relations and show that there is indeed a change in slope around $200\,{\rm km\,s^{-1}}$ in the relations with W and $V_{\rm max}$. We also show that this 'kink' is largely, but not entirely, removed when we use the asymptotic rotation velocity $V_{\rm asymp}$. In section 4, we search for possible explanations for the observed change in slope and show that, when we consider the total baryonic mass (stars + gas) in our galaxies, an entirely linear relation is recovered. Finally, we discuss some implications of our results in section 5.

2 SAMPLE SELECTION AND OBSERVATIONAL DATA

2.1 Sample

We combine data from the three separate studies by Verheijen (2001, V01), Spekkens & Giovanelli (2006, S06) and Noordermeer et al. (2007, N07). The main criteria for inclusion of galaxies from these sub-samples in the present study is that their rotation curves are of good quality and that the maximum and asymptotic rotation velocities are well defined. We thus select the 22 galaxies from V01 with flat or declining rotation curves. For galaxies whose rotation curves rise until the last measured point, the maximum and asymptotic rotation velocities are ill-defined, so we excluded galaxies from V01 with such rotation curves. We include all galaxies from the sample of massive, late-type spiral galaxies from S06, except UGC 2849, which appears to be interacting with a companion and whose kinematics are lopsided. The remaining 7 galaxies have well-defined rotation curves, some of which appear to be weakly declining in the outer regions. However, given the uncertainties in the inclination of the gas layer at large radii, they are also consistent with being entirely flat. Finally, we include all 19 galaxies from N07. These are all early-type disk galaxies (S0 - Sab), and mostly massive ($V_{\rm max} \gtrsim 200\,{\rm km\,s^{-1}}$). Many of these systems have declining rotation curves, with large differences between $V_{\rm asymp}$ and $V_{\rm max}$.

Our final sample consists of 48 galaxies. They are listed, together with the photometric and kinematic data, in table 1.

2.2 Photometric data

We have chosen to study the Tully-Fisher relation using K-band photometry. Near-infrared photometry has a number of clear advantages over conventional optical data. Foremost, the effects of dust extinction is strongly reduced. Several galaxies in our sample are highly inclined with respect to the line of sight, such that a large fraction of the light is absorbed

Table 1. Photometric and kinematic properties used for the Tully-Fisher analysis: (1) galaxy name; (2) total apparent K-band magnitude and error, taken from T96 (Verheijen's galaxies) and the 2MASS galaxy catalogue (Spekkens' and Noordermeer's galaxies); (3) correction for galactic foreground extinction, taken from Schlegel et al. (1998); (4) correction for internal extinction, calculated using equation 1; (5) assumed distance; (6) magnitude error due to distance uncertainty; (7) resulting absolute magnitude; (8) maximum and (9) asymptotic rotation velocities from the rotation curve and (10) width of global HI profile, corrected for instrumental broadening, random gas motions and inclination.

galaxy	m_K	$A_K^{\rm fg}$	A_K^i	D	$\delta M_{\rm dist}$	M_K^c	$V_{\rm max}$	$V_{\rm asymp}$	$W_{20,R}^{c,i}$
	mag			Mpc	mag		km s^{-1}		
(1)	(2)	(3)	(4)	(5)	(6)	(7)	(8)	(9)	(10)
Galaxies from Verheijen (2001)									
UGC 6399	11.09 ± 0.08	0.07	0.06	18.6	0.17	-20.33	88 ± 5	88 ± 5	172 ± 2
UGC 6446	11.5 ± 0.08	0.07	0.02	18.6	0.17	-19.88	82 ± 4	82 ± 4	174 ± 8
NGC 3726	7.96 ± 0.08	0.07	0.05	18.6	0.17	-23.45	162 ± 9	162 ± 9	330 ± 9
NGC 3729	8.6 ± 0.08	0.05	0.03	18.6	0.17	-22.78	151 ± 11	151 ± 11	295 ± 14
UGC 6667	10.81 ± 0.08	0.07	0.10	18.6	0.17	-20.65	86 ± 3	86 ± 3	167 ± 2
NGC 3877	7.75 ± 0.08	0.10	0.15	18.6	0.17	-23.76	167 ± 11	167 ± 11	335 ± 6
NGC 3917	9.08 ± 0.08	0.09	0.12	18.6	0.17	-22.40	135 ± 3	135 ± 3	275 ± 3
NGC 3949	8.43 ± 0.08	0.09	0.05	18.6	0.17	-22.98	164 ± 7	164 ± 7	320 ± 8
NGC 3953	7.03 ± 0.08	0.13	0.08	18.6	0.17	-24.41	223 ± 5	223 ± 5	446 ± 5
UGC 6917	10.3 ± 0.08	0.12	0.04	18.6	0.17	-21.10	104 ± 4	104 ± 4	224 ± 7
NGC 3992	7.23 ± 0.08	0.13	0.08	18.6	0.17	-24.21	272 ± 6	242 ± 5	547 ± 13
NGC 4013	7.68 ± 0.08	0.07	0.15	18.6	0.17	-23.83	195 ± 3	177 ± 6	377 ± 1
NGC 4010	9.22 ± 0.08	0.11	0.17	18.6	0.17	-22.31	128 ± 9	128 ± 9	254 ± 1
UGC 6983	10.52 ± 0.08	0.12	0.03	18.6	0.17	-20.87	107 ± 7	107 ± 7	222 ± 4
NGC 4085	9.2 ± 0.08	0.08	0.11	18.6	0.17	-22.27	134 ± 6	134 ± 6	247 ± 7
NGC 4088	7.46 ± 0.08	0.09	0.10	18.6	0.17	-24.00	173 ± 14	173 ± 14	362 ± 5
NGC 4100	8.02 ± 0.08	0.10	0.14	18.6	0.17	-23.48	195 ± 7	164 ± 13	386 ± 5
NGC 4102	7.86 ± 0.08	0.09	0.07	18.6	0.17	-23.57	178 ± 11	178 ± 11	393 ± 10
NGC 4138	8.19 ± 0.08	0.06	0.05	18.6	0.17	-23.22	195 ± 7	147 ± 12	374 ± 16
NGC 4157	7.52 ± 0.08	0.09	0.20	18.6	0.17	-24.04	201 ± 7	185 ± 10	398 ± 4
NGC 4183	9.76 ± 0.08	0.06	0.14	18.6	0.17	-21.74	115 ± 6	109 ± 4	228 ± 2
NGC 4217	7.61 ± 0.08	0.08	0.15	18.6	0.17	-23.90	191 ± 6	178 ± 5	381 ± 5
Galaxies from Spekkens & Giovanelli (2006)									
NGC 1324	9.15 ± 0.11	0.02	0.18	74.2	0.08	-25.40	305 ± 7	275 ± 9	604 ± 15
ESO 563G21	8.89 ± 0.11	0.08	0.22	59.2	0.10	-25.27	310 ± 11	300 ± 6	655 ± 12
NGC 2862	9.27 ± 0.11	0.01	0.22	55.9	0.10	-24.70	280 ± 5	250 ± 10	574 ± 11
NGC 2955	10.04 ± 0.11	0.00	0.08	95.3	0.06	-24.93	265 ± 19	230 ± 17	546 ± 34
IC 4202	10.41 ± 0.11	0.01	0.23	97.2	0.06	-24.76	245 ± 3	245 ± 3	517 ± 10
NGC 6195	10.18 ± 0.11	0.01	0.09	123.3	0.05	-25.38	255 ± 17	255 ± 17	536 ± 37
UGC 11455	9.23 ± 0.11	0.07	0.26	75.7	0.08	-25.50	280 ± 9	270 ± 10	602 ± 10
Galaxies from Noordermeer et al. (2007)									
UGC 624	9.26 ± 0.11	0.02	0.11	65.1	0.09	-24.94	300 ± 16	270 ± 30	599 ± 38
UGC 2487	8.64 ± 0.11	0.07	0.04	67.4	0.09	-25.61	390 ± 21	330 ± 24	755 ± 36
UGC 2916	10.01 ± 0.11	0.10	0.02	63.5	0.09	-24.13	220 ± 17	180 ± 17	501 ± 39
UGC 2953	6.04 ± 0.11	0.15	0.06	15.1	0.38	-25.07	315 ± 9	260 ± 16	603 ± 18
UGC 3205	9.50 ± 0.11	0.20	0.11	48.7	0.12	-24.24	240 ± 7	210 ± 5	451 ± 7
UGC 3546	8.48 ± 0.11	0.03	0.05	27.3	0.21	-23.78	260 ± 65	190 ± 12	421 ± 13
UGC 3580	10.12 ± 0.11	0.02	0.05	19.2	0.30	-21.37	127 ± 5	125 ± 5	246 ± 7
UGC 3993	10.33 ± 0.11	0.02	0.01	61.9	0.09	-23.66	300 ± 45	250 ± 40	550 ± 79
UGC 4458	9.31 ± 0.11	0.01	0.02	64.2	0.09	-24.76	490 ± 75	240 ± 43	620 ± 93
UGC 4605	8.46 ± 0.11	0.02	0.14	20.9	0.28	-23.30	225 ± 5	185 ± 4	412 ± 2
UGC 5253	7.36 ± 0.11	0.01	0.03	21.1	0.27	-24.30	255 ± 20	210 ± 21	495 ± 34
UGC 6786	8.70 ± 0.11	0.01	0.11	25.9	0.22	-23.48	230 ± 5	215 ± 10	456 ± 6
UGC 6787	7.66 ± 0.11	0.01	0.08	18.9	0.31	-23.82	270 ± 10	250 ± 7	495 ± 7
UGC 8699	9.74 ± 0.11	0.00	0.13	36.7	0.16	-23.22	205 ± 6	180 ± 9	382 ± 10
UGC 9133	8.80 ± 0.11	0.01	0.06	54.3	0.11	-24.94	300 ± 15	225 ± 12	537 ± 18
UGC 11670	7.72 ± 0.11	0.08	0.09	12.7	0.46	-22.97	190 ± 5	160 ± 6	341 ± 6
UGC 11852	10.69 ± 0.11	0.03	0.05	80.0	0.07	-23.90	220 ± 16	165 ± 11	401 ± 29
UGC 11914	6.83 ± 0.11	0.03	0.01	14.9	0.39	-24.08	305 ± 43	–[†]	583 ± 85
UGC 12043	10.81 ± 0.11	0.02	0.05	15.4	0.38	-20.21	93 ± 6	90 ± 4	185 ± 3

[†]The rotation curve of UGC 11914 only extends out to about 3.3 R-band disk scale lengths and does not show the characteristic decline that is seen in other galaxies of similar type and luminosity (see N07). Since in many comparable cases, the decline in the rotation velocities sets in outside the optical disk only, it is well possible that the rotation curve in UGC 11914 would also decline at larger radii if we were able to measure it. The asymptotic rotation velocity $V_{\rm asymp}$ for UGC 11914 seems therefore ill-defined and we excluded this galaxy from the sample for the asymptotic velocity relations.

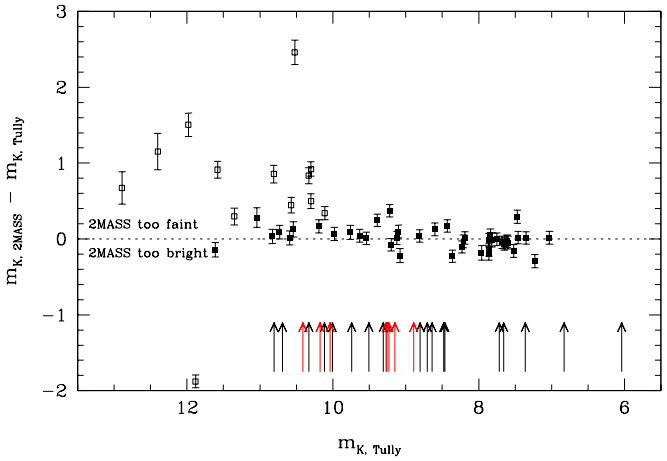

Figure 1. Comparison of 2MASS K-band magnitudes with the data from T96. Data points show the difference between the total apparent magnitudes from 2MASS and those from T96; errorbars show the combined errors. Open symbols indicate low surface brightness galaxies ($\mu_{0,K} > 18$ mag arcsec^{-2}), filled symbols indicate HSB systems. Black and red vertical arrows indicate the 2MASS apparent magnitudes for the galaxies from N07 and S06 respectively.

by internal dust. In the optical bands, this effect can be very significant ($\gtrsim$ 1mag), leading to large uncertainties in the derived absolute luminosities. In the near infrared, these uncertainties are less severe. In addition, recent bursts of star formation can have a large effect on the optical luminosity of a galaxy, whereas the K-band is much less sensitive to such events.

Deep K-band photometry for the galaxies from V01 is available from Tully et al. (1996, hereafter T96). Neither S06 nor N07 had private near-infrared photometry at their disposal, but all galaxies from these subsamples have been observed in K in the framework of the Two Micron All Sky Survey[1]. Although 2MASS is a very homogeneous survey, it is also less deep than the data from T96. To judge the reliability of the 2MASS photometric data, and to ensure that we do not introduce systematic differences between our various subsamples, we compared the K-band magnitudes from T96 with the total extrapolated magnitudes from 2MASS, for all systems which were detected in both surveys.

Figure 1 shows that there is good agreement between the 2MASS photometry and Tully's data for high surface brightness (HSB) galaxies. For the galaxies with measured central surface brightness $\mu_{0,K} < 18.0$ mag arcsec^{-2}, the average difference between 2MASS' and T96's magnitudes is 0.01 mag, with a standard deviation of 0.14 mag. V01 reported, based on an internal comparison of their observations from different nights, an average photometric uncertainty of 0.08 mag in the K-band magnitudes of T96. This implies that the uncertainties in the 2MASS magnitudes must be approximately 0.11 mag, significantly larger than the average errors given by the 2MASS database (typically 0.03 mag for the HSB galaxies in figure 1). Photometric errors of 0.03 mag seem somewhat optimistic, in particular since the 2MASS images are significantly less deep than those of T96.

Figure 1 also shows that for low surface brightness galaxies, the 2MASS magnitudes are not reliable and sometimes deviate strongly from the values from T96. Inspection of the 2MASS images for these galaxies shows that they are of such low surface brightness that they are often barely detected (in fact, most of the LSB galaxies from Tully's sample are not detected at all by 2MASS). It appears that 2MASS has missed a large fraction of the flux of many LSB galaxies, compared to the deeper data from T96.

The galaxies from N07 and S06 are all luminous, high surface brightness galaxies. For these objects, it seems safe to adopt the 2MASS magnitudes, but we assume an average photometric uncertainty of 0.11 mag instead of the smaller errors given by 2MASS.

To convert the apparent magnitudes to absolute luminosities, we first correct for extinction effects. Corrections for Galactic foreground extinction were taken from Schlegel et al. (1998); they are generally small ($\leqslant$ 0.1 mag for 85% of the galaxies). Several correction schemes exist to determine the amount of *internal* extinction; the most commonly used methods are based on those of Tully & Fouqué (1985) or Giovanelli et al. (1994). Here, we follow V01, who employed the following relation, originally derived by Tully et al. (1998), for the internal extinction parameter:

$$A_\lambda^{i\rightarrow 0} = -\gamma_\lambda \log\left(\frac{b}{a}\right), \qquad (1)$$

with b/a the observed minor-to-major axis ratio of the optical image. γ_λ is wavelength dependent and was found by Tully et al. (1998) to depend also on the absolute luminosity of the galaxy: brighter galaxies contain on average more dust than fainter ones. These authors used the Tully-Fisher relation itself, in an iterative way, to express the absolute luminosity in terms of the HI line width, and give the following description for γ_λ:

$$\gamma_\lambda = \alpha_\lambda + \beta_\lambda(\log W_{20,R}^{c,i} - 2.5), \qquad (2)$$

where $W_{20,R}^{c,i}$ is the HI line width, corrected for inclination and broadening due to instrumental effects and random gas motions (see below). For the wavelength dependent parameters α_λ and β_λ, we use the values given by Tully et al. (1998). Note that even in the K-band used here, we find significant internal extinction corrections, although they do not exceed 0.1 magnitude except in the most inclined systems.

Distances for our galaxies were derived as follows. All galaxies in V01 belong to the Ursa Major cluster and have therefore roughly equal distances; throughout this study, we adopt Verheijen's value of 18.6 Mpc (taken from Tully & Pierce 2000). For the galaxies from N07, we used the distances as derived by Noordermeer et al. (2005), which were based on a simple Hubble-flow model, corrected for Virgo-centric infall and assuming a Hubble constant of 75 km s^{-1} Mpc^{-1}. For the galaxies from S06, we used the same method[2].

[1] 2MASS (http://www.ipac.caltech.edu/2mass/) is a joint project of the University of Massachusetts and the Infrared Processing and Analysis Center/California Institute of Technology, funded by the National Aeronautics and Space Administration and the National Science Foundation.

[2] Note that our distance estimates for the galaxies from S06 are

In table 1, we give for each galaxy the raw apparent magnitudes and photometric errors, the galactic foreground and internal extinction parameters, $A_K^{\rm fg}$ and A_K^i, the assumed distances and the resulting corrected absolute magnitudes used in the remainder of this paper.

Finally, in addition to the photometric errors, we also account for the uncertainties in the absolute magnitudes which arise from errors in our distance estimates. For the galaxies from V01, these are defined by the depth of the Ursa Major cluster; here, we adopt Verheijen's estimate of 0.17 mag. For the other galaxies, we estimate the distance uncertainties by assuming a typical peculiar velocity of $200\,{\rm km\,s^{-1}}$. The resulting errors on the absolute magnitude $\delta M_{\rm dist}$ are given in column (7) of table 1 and were added quadratically to the photometric errors to obtain the total uncertainties used for the subsequent analysis.

Note that we have not included the uncertainties in the internal extinction corrections in our error budget here. Especially for the highly-inclined systems in our samples, the corrections A_λ^i are significant and galaxy-to-galaxy variations of γ_λ can cause substantial deviations from the corrections used here. However, without additional information about the dust content of our galaxies, the corrections listed in table 1 are the best possible estimate and the uncertainties are very difficult to quantify. We will ignore these uncertainties for the subsequent analysis here, but note that some of the scatter in our TF relations might be explained by the uncertainties in the internal extinction.

2.3 Kinematic data

We use three kinematic parameters for our Tully-Fisher analysis. The first is the inclination corrected width of the HI line profile. For this, we used the instrumental broadening corrected measurements from Verheijen & Sancisi (2001), S06 and Noordermeer et al. (2005) respectively. We apply an additional correction for broadening of the profiles caused by random gas motions in the gas disks, using the prescriptions given by Verheijen & Sancisi (2001, based on Tully & Fouqué 1985):

$$\left(W_{20,R}^c\right)^2 = \left(W_{20}^c\right)^2 \,+\, W_t^2 \left[1 - 2e^{-\left(\frac{W_{20}^c}{W_c}\right)^2}\right] \,- \\ 2W_{20}^c W_t \left[1 - e^{-\left(\frac{W_{20}^c}{W_c}\right)^2}\right], \qquad (3)$$

with W_{20}^c the profile width corrected for instrumental broadening. W_c indicates the profile width where the transition from a Gaussian to a boxy shape occurs; we assume here $W_c = 120\,{\rm km\,s^{-1}}$ (de Vaucouleurs et al. 1983). In practice, most of our galaxies have profile widths larger than W_c, such that equation 3 yields a linear subtraction of W_t, which gives the amount by which a profile is broadened due to the random gas motions. Verheijen & Sancisi (2001) present an extensive discussion about the suitable choice for W_t; here we simply copy their preferred value of $W_t = 22\,{\rm km\,s^{-1}}$. The derived profile widths $W_{20,R}^c$ were corrected for inclination using the values derived in the original papers; for warped galaxies we use the inclination in the inner regions where most of the gas is concentrated.

The two other kinematic parameters are the maximum rotation velocity $V_{\rm max}$ and the asymptotic rotation velocity $V_{\rm asymp}$ ($V_{\rm flat}$ in V01), which are both derived directly from the rotation curves.

For the galaxies from V01, we copied the errors on the kinematic parameters without further modification. For the galaxies from N07, we used the inclination uncertainty derived in the original paper to estimate the errors on the profile widths. The errors on the two other kinematic parameters were estimated by eye, based on the errors in the rotation curves. The latter include contributions from measurement errors, kinematic asymmetries and inclination uncertainties; for the more face-on galaxies, the latter are usually dominant. Finally, for the galaxies from S06, we used the uncertainty in the ellipticity of the optical images, given in the original paper, to estimate the inclination uncertainty, but adopted a minimum of 5° to account for the possibility of undetected warps in the outer parts of the gas layer. The errors on $V_{\rm max}$ and $V_{\rm asymp}$ were again estimated by eye, based on the errors in the rotation curves.

All three kinematic parameters and corresponding errors for each galaxy are given in table 1.

3 TULLY-FISHER RELATIONS

In figure 2, we show the Tully-Fisher relations for the combined sample of galaxies. Compared to the study in V01, our combined sample greatly increases the number of luminous galaxies, with our most luminous system, UGC 2487, being 1.2 magnitudes brighter than the most luminous object in Verheijen's sample.

We fitted direct linear relations of the following form to the combined data sets:

$$M_K^c = M_{2.6} + S\,(\log W - 2.6)\,, \qquad (4)$$

where M_K^c is the extinction corrected absolute magnitude and W is either $W_{20,R}^{c,i}$, $2V_{\rm max}$ or $2V_{\rm asymp}$. We calculated the zeropoint $M_{2.6}$ at $\log W = 2.6$, rather than 0, to avoid strong covariances between the two free parameters. The fits were done using a simple χ^2-minimisation procedure, taking the errors in both directions into account. They are indicated with the magenta lines in figure 2; for comparison, we also show (in black) the fits to the 'F'-sample from V01, i.e. the fits made to galaxies with flat rotation curves only.

The results of the fits to the combined sample are summarised in table 2. The scatter around each of the fits given in this table is a weighted rms scatter, with the weight for each data point given by $w_i = (\sigma_{M,i}^2 + S^2\sigma_{\log W,i}^2)^{-1}$. Here, $\sigma_{M,i}$ are the magnitude errors, $\sigma_{\log W,i}$ are the errors in the parameters on the x-axes and S are the fitted slopes of the relations.

A number of interesting results can be recognised from figure 2 and table 2. First of all, our data strongly suggest a 'kink' in the Tully-Fisher relation: the TF relation

slightly different from those given in the original paper. Part of the discrepancy comes from the fact that we assume $h = 0.75$ instead of 0.70. Further differences arise from the treatment of Virgo-centric streaming motions, but are small (< 0.1 mag in all cases).

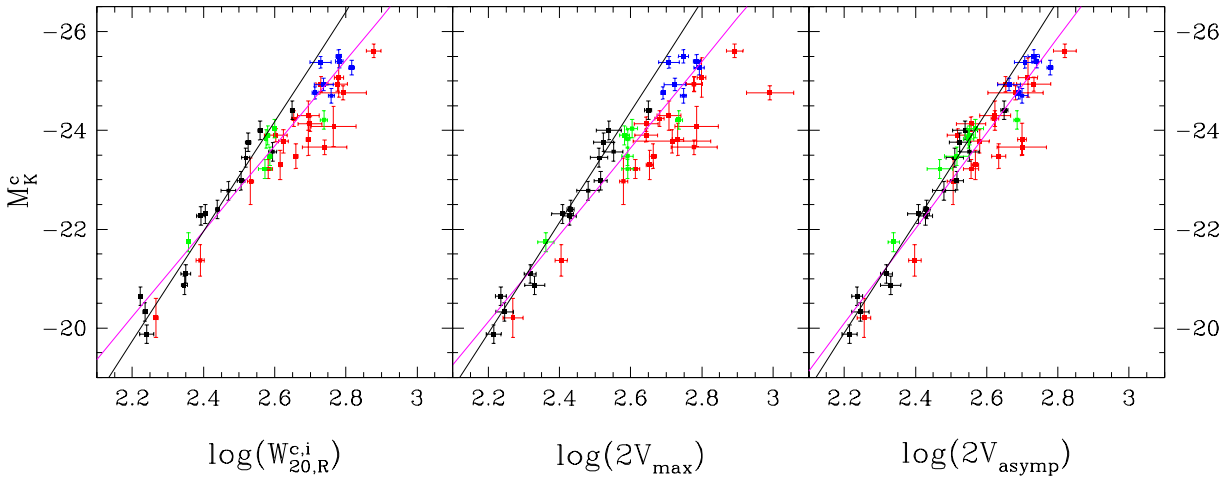

Figure 2. Tully-Fisher relations in the K-band, using the corrected widths of the global HI profiles (*left*) and the maximum (*middle*) and asymptotic rotation velocities (*right*). Black and green data points show galaxies from V01 with flat and declining rotation curves respectively; blue data points show galaxies from S06 and red points show galaxies from N07. The black lines show the fits from V01 to galaxies with flat rotation curves, while the magenta lines show the fits to the combined sample (see table 2).

Table 2. Results from the least-χ^2 fits to the K-band Tully-Fisher relations shown in figure 2.

kinematic parameter	# of points	$M_{2.6}$	S	scatter	$\chi^2_{\rm red}$	Q
		mag		mag		
$W^{c,i}_{20,R}$	48	-23.69 ± 0.03	-8.65 ± 0.19	0.38	2.89	$3.3 \cdot 10^{-11}$
$V_{\rm max}$	48	-23.64 ± 0.04	-8.77 ± 0.22	0.44	2.98	$7.2 \cdot 10^{-12}$
$V_{\rm asymp}$	47	-23.95 ± 0.04	-9.64 ± 0.25	0.36	1.76	$5.4 \cdot 10^{-4}$
$V_{\rm asymp}$ (UGC 3993 and 6787 excluded)	45	-23.97 ± 0.04	-9.71 ± 0.26	0.34	1.54	$6.8 \cdot 10^{-3}$

seems to become shallower above a rotation velocity of about $200\,{\rm km\,s^{-1}}$ (equivalent to $M_K^c \approx -23.75$). This is consistent with the claim first made by Peletier & Willner (1993), but the effect is much more clearly visible here than in their data. The kink is most apparent when using the width of the global profile ($W^{c,i}_{20,R}$) or the maximum rotation velocity $V_{\rm max}$ as kinematic parameter. In the left and middle panels in the figure, almost all galaxies from the S06 and N07 samples lie to the right of the relation defined by the intermediate-mass galaxies with flat rotation curves from V01. As a result, the fits to the combined samples have a shallower slope than those from Verheijen to the galaxies with flat rotation curves. In particular, many of the massive, early-type disk galaxies from N07 lie far away from the relation defined by the later-type spirals from Verheijen and S06; when expressed in terms of a luminosity offset, their distance from the main relation can be as large as 2 magnitudes.

However, the turnover is greatly reduced when using the asymptotic rotation velocity $V_{\rm asymp}$ as kinematic parameter. Many of the galaxies in our sample with $V_{\rm max} > 200\,{\rm km\,s^{-1}}$, in particular the early-type disks from N07, have strongly declining rotation curves. Galaxies such as UGC 4458, 4605, 3546, which lie far to the right of the main relation in the left and middle panels, shift to the left when the (lower) asymptotic velocity is used, thereby straightening the TF relation. This effect is also reflected in the values for the rms scatter and χ^2 of the data around the fits and the 'goodness-of-fit' parameters Q. Table 2 shows that the TF relations using $V_{\rm asymp}$ are much better represented by straight lines than the relations with the other two parameters.

It is important, however, to note that the kink does not disappear completely when using $V_{\rm asymp}$ as kinematic parameter. Even in the right hand panel of figure 2, most galaxies at the bright end lie to the right of the relation defined by the less luminous galaxies with flat rotation curves from V01, indicating that the slope of the TF relation also changes when the asymptotic rotation velocities $V_{\rm asymp}$ are used. This is also confirmed when we fit linear relations to the subsamples of galaxies fainter and brighter than $M_K^c \approx -24$; in this case, we find that the slope changes significantly, from -10.5 ± 0.5 to -7.7 ± 0.9 respectively.

The scatter in our relation using the asymptotic rotation velocities is systematically larger than the corresponding value found by V01. This difference can partly be attributed to the fact that Verheijen's galaxies all lie in the Ursa-Major cluster, such that the distance uncertainties are small (at least in a relative sense). The galaxies from S06 and N07 lie predominantly in the field, where peculiar motions with respect to the Hubble flow lead to errors in the derived distances and absolute luminosities (see table 1), and thus to additional scatter in the TF relations. More importantly however, the scatter in our relations is artificially increased by the deviations from a straight line. Even in the relations using the asymptotic rotation velocity $V_{\rm asymp}$, the kink around $200\,{\rm km\,s^{-1}}$ causes systematic deviations from the fitted straight lines. Since V01 had only 2 galaxies with $V_{\rm asymp} > 200\,{\rm km\,s^{-1}}$, the change in slope at the high mass

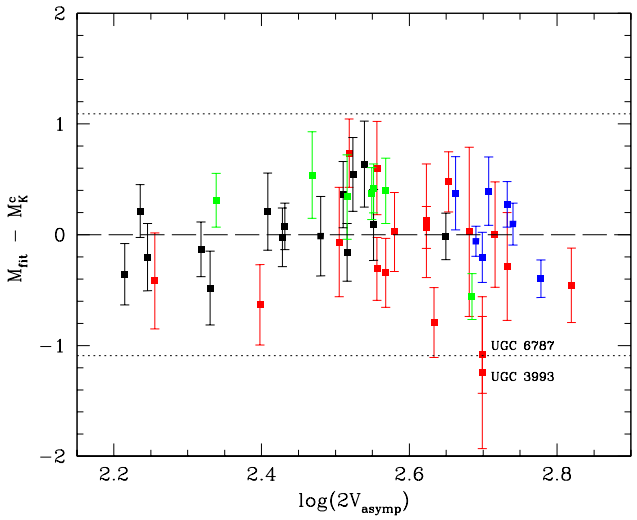

Figure 3. Deviations of our objects with respect to the K-band vs. $V_{\rm asymp}$ TF relation from table 2. Symbol colours are the same as in figure 2. Errorbars are the effective errors, calculated by combining the magnitude and velocity uncertainties (see text). Dotted lines indicate the formal 3σ limits.

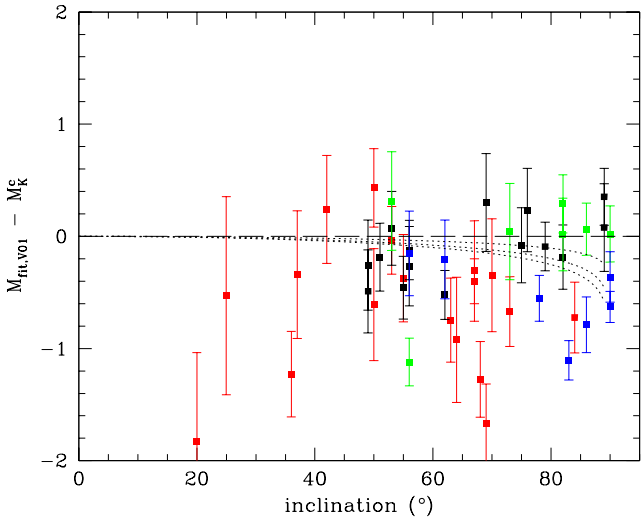

Figure 4. Deviations of our objects with respect to Verheijen's K-band vs. $V_{\rm asymp}$ TF relation for galaxies with flat rotation curves, as a function of inclination. Symbol colours are the same as in figure 2. The dotted lines show the adopted internal extinction corrrections for fiducial galaxies with HI profile widths of 200, 400 and 600 $\rm km\,s^{-1}$ (top to bottom respectively).

end had virtually no influence on the scatter around the fits for his data.

Finally, the scatter in the relations with $V_{\rm asymp}$ is heavily influenced by two galaxies with unusually large deviations from the main relation: UGC 3993 and UGC 6787 (3.4 and 3.0σ outliers respectively). In figure 3, we show the deviations of the galaxies from our sample with respect to the M_K^c vs. $V_{\rm asymp}$ fit described in table 2. The errorbars in the figure take the uncertainties of the points in both directions into account, and were calculated as $(\Delta\,(M-M_{\rm fit}))^2 = (\Delta M)^2+(\Delta \log(2V)\cdot S)^2$, with $S=-9.64$ the slope of the fit.

UGC 3993 is a nearly face-on galaxy ($i \approx 20°$, see N07), with correspondingly large uncertainties in the derived rotational velocities (also reflected in the large errorbars in figures 2 and 3). The deviation of this galaxy may be due partly to a slight under-estimation of the true inclination angle. It seems unlikely, however, that the inclination uncertainty is responsible for the full deviation of UGC 3993; to bring this galaxy to the middle of the relation would require an inclination angle of 30°, a value which seems to fall outside the range supported by the observational data (see N07).

The most likely explanation for the offset of UGC 6787 from the main relation lies in the distance determination. UGC 6787 lies close to the center of the Ursa Major cluster, but has a redshift that is about $200\,\rm km\,s^{-1}$ higher than the high velocity envelope of the cluster (Tully et al. 1996). It may thus lie behind the main cluster, which might in turn imply that it is being drawn into the cluster and that the recession velocity is lower than expected in the case of pure Hubble flow. In that case, our adopted distance of 18.9 Mpc and the derived luminosities are too small, explaining the offset in the TF relations.

For completeness, we also list in table 2 the results of fits to the TF relations with the asymptotic rotation velocities when UGC 3993 and 6787 are excluded from the sample. It is clear that the exclusion of the two points from the fits does not lead to significantly different slopes or zeropoints. As expected, the scatter is reduced, but since the kink in the relations has not been removed by the exclusion of the two discrepant points, the values are still larger than the corresponding ones from V01 and the χ^2 and Q-parameter indicate that the deviations from a straight relation are still real.

4 DISCUSSION

4.1 Systematic variations along the TF relation

What could be the origin of the change of slope in the Tully-Fisher relation? Does it truly indicate a break in the relation between baryons and dark matter, or could it be explained by other effects? An obvious possibility is that some of the corrections from sections 2.2 and 2.3 are inaccurate for the brightest galaxies. Such an effect may lead to a systematic deviation of these galaxies from the TF relation for lower-mass galaxies, precisely as observed.

4.1.1 internal extinction

The largest uncertainty in the corrections which we applied to our raw data lies, most probably, in the treatment of the internal extinction. We corrected for internal extinction following Tully et al. (1998). They derived their corrections from a sample of galaxies which spans a roughly similar luminosity range as ours and, importantly, observed no systematic deviations of the brightest galaxies. On the other hand, Giovanelli et al. (1995) *did* find a hint for excess extinction in the brightest spirals. Given the uncertainties, it is useful to explicitly verify whether the deviations of our most massive galaxies with respect to the TF relation for

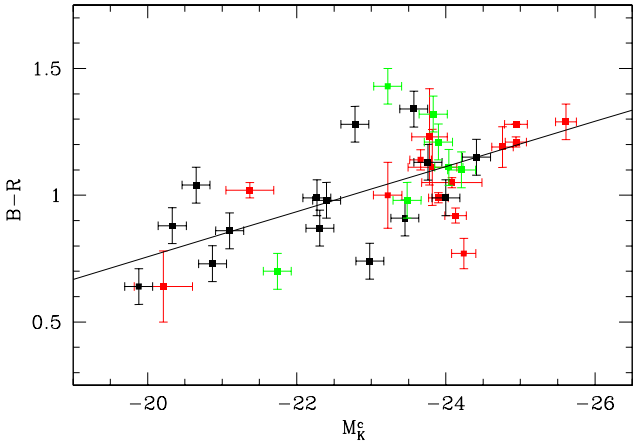

Figure 5. Colour-magnitude relation for all galaxies in our sample for which B-R colours are available. Colour information for galaxies from V01 were taken from the same paper, whereas Noordermeer & van der Hulst (2007) give colours for a subset of the galaxies from N07. The black line shows a least-squares linear fit to the data points.

low- and intermediate-mass galaxies can be explained as being due to an underestimation of the internal extinction in these systems. This is done in figure 4, where we plot the deviations of all galaxies with respect to Verheijen's TF relation for spirals with flat rotation curves, as a function of inclination.

Figure 4 shows a tentative trend for the galaxies from S06 (blue points), with the edge-on systems deviating more than the galaxies with intermediate inclinations. To explain this trend, about a factor three more extinction is required in these galaxies than assumed in section 2.2. The galaxies from N07 (red points), however, do not follow an obvious trend and strongly deviating cases are found among both near-face-on and highly-inclined galaxies.

Based on our data, we cannot strictly rule out the possibility that the internal extinction in the most massive spiral galaxies is higher than we assumed. However, figure 4 shows that if this is indeed the case, it still cannot explain the deviations of the low-inclination galaxies. It therefore seems unlikely that the change of slope at the high-mass end of the Tully-Fisher relation can be explained purely as an effect of excess extinction in the most massive disk galaxies.

4.1.2 stellar population variations

Another possibility which could explain a change of slope in the Tully-Fisher relation is that the most massive galaxies have stellar populations with higher mass-to-light ratios than the less luminous systems, such that they are underluminous for a given rotation velocity. To first order, such an effect is likely to be present in disk galaxies, given the well-known fact that bright galaxies tend to be redder than their less-luminous counterparts (Visvanathan 1981; Tully et al. 1982). This colour-magnitude relation is also present in our own sample: in figure 5, we plot the B-R colours as a function of absolute luminosity, for the subset of our galaxies for which the former are available.

The colour-magnitude relation itself cannot, however, be responsible for the kink in the TF relation. Figure 5 shows that the colour changes linearly with absolute magnitude. Since mass-to-light ratio changes exponentially with colour (Bell & de Jong 2001), this gradient will translate in a linear effect in the Tully-Fisher relation. In other words, a linear colour-magnitude relation will introduce a change in the *global* slope of the Tully-Fisher relation. Specifically, using the fitted slope of the colour-magnitude relation in figure 5, in conjunction with the slope of the colour vs. mass-to-light ratio relation from Bell & de Jong, it can be derived that the stellar *mass* Tully-Fisher relation will be 10% steeper than the relations shown in figure 2 and table 2. Importantly, however, a linear colour-magnitude relation cannot introduce a turnover in the TF relation. Only a break in the colour-magnitude relation at the same luminosity as the kink in the TF relation can explain the latter, but figure 5 shows that such a feature is not present in our sample.

4.2 The Baryonic Tully-Fisher relation

Having established that the observed change of slope in our K-band vs. $V_{\rm asymp}$ TF relation is not due to variations in internal extinction or the properties of the stellar populations, we now consider whether trends in relative gas content play a rôle. In this context, it is interesting to consider the so-called 'Baryonic Tully-Fisher relation', first discussed by McGaugh et al. (2000, see also McGaugh 2005). They showed that there exists another break in the Tully-Fisher relation at the low luminosity end (around $V_{\rm rot} = 90\,{\rm km\,s^{-1}}$), below which galaxies are also under-luminous. They were, however, able to restore a linear TF relation when, instead of using the stellar luminosity, they adopted the total observed baryonic mass (stars and gas). Since dwarf galaxies contain on average more gas than higher-luminosity spirals (relative to the optical luminosity, e.g. Haynes & Giovanelli 1984; Verheijen & Sancisi 2001; Swaters et al. 2002; Geha et al. 2006), the former shifted upwards more than the latter, and the kink in the Tully-Fisher relation disappeared. Luminous galaxies, on the other hand, generally contain relatively little gas. In particular, in Noordermeer et al. (2005), it was shown that some of the early-type disk galaxies from N07 are very gas-poor. In such galaxies, the baryonic budget is dominated by the stars and adding the gas contribution will not lead to a significant increase in brightness.

We have investigated whether the observed break at the high mass end in our Tully-Fisher relations can be explained as a result of the relatively low gas-content of the most luminous galaxies in our sample. To this purpose, we have converted the total K-band luminosities to stellar masses, assuming an average mass-to-light ratio of the stellar populations of 0.8. The choice of $M_*/L_K = 0.8$ was made following McGaugh et al. (2000), and is consistent with the average values found from maximum-disk fits from Verheijen (1997) and Palunas & Williams (2000). In reality, the values of M_*/L_K are expected to vary from galaxy to galaxy, but the variations will be modest in the K-band and we ignore this variation for the moment. The possibility that the assumption of constant M/L gives rise to additional scatter in the baryonic TF relation is investigated below.

For the gas masses, we used the total HI masses as given by V01, Noordermeer et al. (2005) and S06 respectively, multiplied by 1.43 to account for the presence of he-

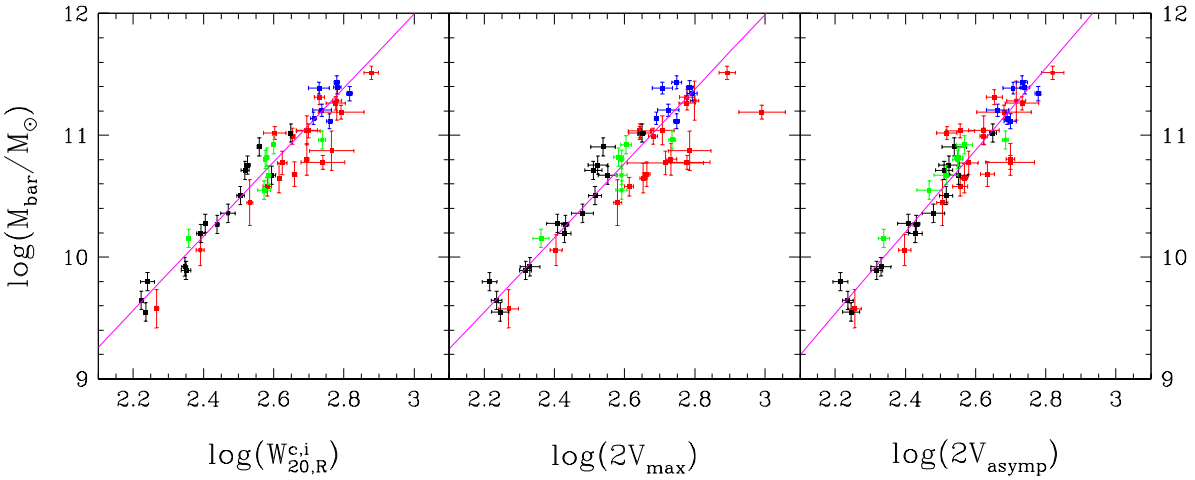

Figure 6. Baryonic Tully-Fisher relation. The total K-band luminosity was converted to stellar mass, assuming a mass-to-light ratio of the stars of 0.8 (see text), and added to the neutral gas mass. Colours of symbols and lines are the same as in figure 2.

Table 3. Results from the least-χ^2 fits to the Baryonic Tully-Fisher relations shown in figure 6.

kinematic parameter	$(\log M)_{2.6}$	S	scatter mag[a]	$\chi^2_{\rm red}$	Q
$W^{c,i}_{20,R}$	10.78 ± 0.01	3.04 ± 0.08	0.32	2.17	$2.2 \cdot 10^{-6}$
$V_{\rm max}$	10.77 ± 0.01	3.05 ± 0.09	0.40	2.57	$2.4 \cdot 10^{-9}$
$V_{\rm asymp}$	10.88 ± 0.02	3.36 ± 0.10	0.36	1.92	$7.7 \cdot 10^{-5}$
$V_{\rm asymp}$ (UGC 3993 and 6787 excluded)	10.89 ± 0.02	3.38 ± 0.10	0.34	1.72	$1.0 \cdot 10^{-3}$

[a]For consistency with table 2, we express the scatter in magnitudes. The scatter in $\log(M_{\rm bar})$, as shown in figure 6, is a factor 2.5 lower.

lium. The stellar and gas masses were then added to obtain an estimate for the total baryonic mass content in our galaxies. The resulting baryonic TF relations are shown in figure 6 for the same three kinematic parameters as used before; the resulting least-χ^2 fits are summarized in table 3.

As expected from the general trends of gas content with total luminosity mentioned above, the baryonic Tully-Fisher relations have a shallower slope than the standard stellar TF relations. But more importantly, the 'kink' in the TF relations from figure 2 is reduced. The relations with $W^{c,i}_{20,R}$ and $V_{\rm max}$ are better represented by a straight line than the original relations in figure 2; the scatter and χ^2 are reduced with respect to the original values and the Q-parameters are higher. Thus, our data show that the concept of the Baryonic Tully-Fisher relation is not only useful to increase the linearity in the TF relation at the low luminosity end, but that in addition, it also reduces the kink around 200 km s^{-1}. However, this effect is smaller than the one discussed in the previous section, and the Baryonic Tully Fisher relations using $W^{c,i}_{20,R}$ or $V_{\rm max}$ are still worse than our original, *stellar* luminosity vs. $V_{\rm asymp}$ relation shown in figure 2 and table 2.

The inclusion of the gas does, however, remove the small kink that was still present in the latter relation as well, and the baryonic mass vs. $V_{\rm asymp}$ TF relation appears to be consistent with a linear relation over the full extent of our data. However, at the same time, the scatter around the mean relation does not appear to have decreased and the formal quality of the fit, as measured with the χ^2 and Q-parameter, is actually reduced.

The scatter might be reduced if more accurate K-band mass-to-light ratios become available for individual galaxies instead of the constant value of $M_*/L_K = 0.8$ we assumed here. We investigate this possibility in figure 7, where we plot the deviation of each galaxy with respect to the bary-

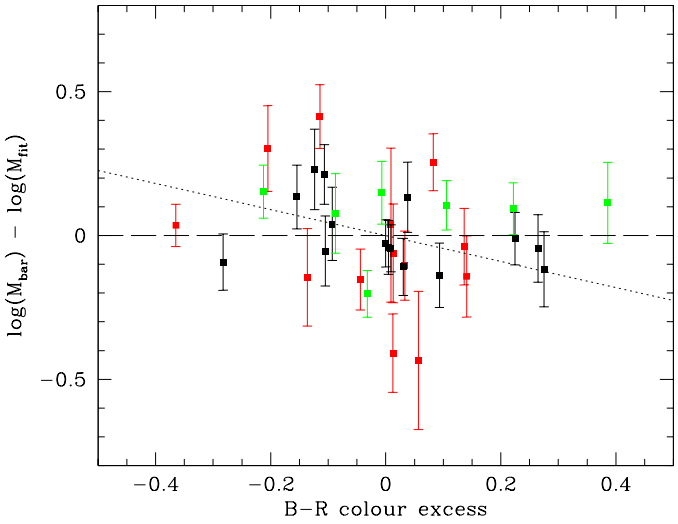

Figure 7. Deviations of our objects with respect to the baryonic mass vs. $V_{\rm asymp}$ TF relation, as a function of the colour excess of each galaxy with respect to the linear fit shown in figure 5. Symbol colours are the same as in figure 2. The dotted line shows the behaviour predicted by the stellar population synthesis models from Bell & de Jong (2001).

onic mass vs. $V_{\rm asymp}$ TF relation, as a function of its colour excess with respect to the linear fit shown in figure 5. As discussed in section 4.1.2, the global colour-magnitude trend only leads to a change in slope of the TF relation. The deviations from this global trend, however, are expected to give rise to additional scatter in the TF relation, hence the use of the colour *excess* on the abscissa.

It is clear from figure 7 that there is little relation between the offsets from the baryonic TF relation and the colours. In particular, the data points do not follow the trend as predicted on the basis of the stellar populations synthesis models from Bell & de Jong (2001). Given the uncertainties in these models and in our own data, we cannot yet rule out the possibility that part of the scatter in the baryonic Tully-Fisher relation *is* related to variations in the mass-to-light ratios, but the current data suggest that this is not the main contribution. Thus, most of the scatter in the baryonic Tully-Fisher relation must be related to other observational effects, or be intrinsic.

Note that the value of the χ^2 parameter for the baryonic $V_{\rm asymp}$ TF relation (1.92 or 1.72, depending on whether or not the outlying UGCs 3993 and 6787 are included in the fit) implies that roughly 50% of the scatter in this relation results from the observational uncertainties in the data points. This leaves an upper limit of approximately 0.25 magnitude ($\approx 25\%$ luminosity) for the intrinsic TF scatter in our galaxies. Given the fact that we have not included the uncertainties in the internal extinction corrections or the mass-to-light ratios in our errorbars and that there may well be additional uncertainties which we have ignored, it seems safe to assume that this is a conservative upper limit and that the intrinsic TF scatter is very small indeed.

5 CONCLUDING REMARKS

In this study, we have used K-band photometry and high-quality rotation curves to show that there is a 'break' in the Tully-Fisher relation around a rotation velocity of about $200\,{\rm km\,s^{-1}}$ (equivalent to $M_K^c \approx -23.75$, or $M_* \approx 0.7\times10^{11}{\rm M}_\odot$), above which most galaxies rotate faster than expected (or equivalent, are less luminous). This kink is most pronounced in the traditional formulations of the TF relation, using stellar luminosities and the widths of the HI profiles or the maximum rotational velocities, and we have shown that it is mainly due to massive early-type disk galaxies with declining rotation curves, which lie systematically to the right of the relation defined by less massive and later-type spiral galaxies. The kink is also present, albeit to a lesser extent, in the relation with the asymptotic rotation velocity at large radii. In this case, there is no systematic offset between early- and late-type spirals, and the change in slope appears independent of morphological type.

It is important to note that the 'elliptical galaxy Tully-Fisher relation' (using circular velocities derived from dynamical models, rather than direct observations) shows a similar change in slope, at approximately the same location (Gerhard et al. 2001; de Rijcke et al. 2007). Thus, the change in slope of the stellar luminosity vs. circular velocity relation appears to hold universally and along the entire Hubble sequence. Note, however, that due to the limited spatial extent of the dynamical tracers in elliptical galaxies, it is not generally possible to measure the asymptotic rotation velocity in these systems. It can therefore not be ruled out that the kink in the elliptical galaxy TF relation would (partly) disappear if one could use the circular velocity at radii comparable to the outer edges of the HI disks in spiral galaxies.

A change in slope at the high-luminosity end has important consequences for the use of the Tully-Fisher relation as a tool for estimating distances to galaxies or for probing galaxy evolution. In recent years, many studies have addressed the evolution of the Tully-Fisher relation on cosmological timescales (i.e. between $z \approx 1$ and 0), although the results are still somewhat ambiguous. In their pioneering studies, Vogt et al. (1996, 1997) reported that galaxies at redshift $z \sim 1$ were on average 0.6 mag brighter (B-band) than galaxies in the local universe. Other authors find much larger luminosity evolution (Milvang-Jensen et al. 2003; Bamford et al. 2006), up to 1.5 – 2 magnitudes at redshifts of 0.25 – 0.45 (Rix et al. 1997; Simard & Pritchet 1998), whereas it has also been claimed recently that this is all due to observational effects, and that in reality, there has been no luminosity evolution whatsoever (Flores et al. 2006). Given the uncertainties in the measured zeropoint offsets, it is not surprising that measurements of evolution in the TF slope disagree as well. Ziegler et al. (2002), Böhm et al. (2004) and Böhm & Ziegler (2006) claimed that the evolution in the Tully-Fisher relation is luminosity dependent, with high mass galaxies ($V_{\rm max} > 150\,{\rm km\,s^{-1}}$) showing little or no evolution, but low mass galaxies being up to 2 magnitudes brighter at high redshift. In contrast, Weiner et al. (2006) found that massive galaxies evolve more than fainter ones.

Whatever concensus will be reached eventually, the presence of a change of slope in the local TF relation needs to be taken into account when interpreting the observed evolution. Our results indicate that high mass galaxies are *under*-luminous in the local universe, compared to a simple extrapolation of the linear relation for lower-luminosity galaxies. This offset is strongest for early-type disks, i.e. galaxies with a high-surface brightness bulge, and for the TF relation based on the maximum rotation velocity $V_{\rm max}$. Crucially, high-redshift studies will often be biased towards such high-surface brightness galaxies. Moreover, when based on optical spectroscopic measurements, they will not be able to detect a declining rotation curve at large radii, and thus be forced to use $V_{\rm max}$, rather than $V_{\rm asymp}$. These two selection effects, when applied to our own data, give rise to an offset of high-mass galaxies from the main relation, defined by low-mass galaxies with flat rotation curves, of $1-2$ magnitudes (middle panel in figure 2). Thus, the luminosity evolution of high mass galaxies may be much larger than derived by the authors mentioned above.

We have also shown that the 'kink' in the TF relation can be reduced in two different ways, namely *1*) by using the asymptotic rotation velocity from the rotation curve as kinematic parameter and *2*) by using the total baryonic mass (stars + gas) rather than luminosity. The first correction appears to be the most important one for high mass galaxies and the TF relations using the asymptotic rotation velocities show only a small deviation from linearity. However, the inclusion of the gas mass also improves the linearity and only when both refinements are used in conjunction does

the 'kink' disappear completely and is a linear relation recovered.

It is, again, interesting to note that the kink in the elliptical galaxy TF relation also disappears when using the total baryonic mass rather than stellar luminosity (Gerhard et al. 2001; de Rijcke et al. 2007), so that galaxies along the entire Hubble sequence appear to follow the same, linear, baryonic TF relation. Our results seem a strong confirmation of the idea that the baryonic Tully-Fisher relation is fundamentally a relation between the mass of the dark matter haloes (which define $V_{\rm asymp}$) and the total baryonic mass in galaxies and that it holds universally, regardless of how the baryons are distributed within the haloes (cf. McGaugh et al. 2000; Verheijen 2001).

ACKNOWLEDGEMENTS

We would like to thank Kristine Spekkens for kindly providing the rotation curves for her rapidly rotating late-type spiral galaxies and for stimulating discussions which helped to significantly improve the paper. We are also grateful to Thijs van der Hulst, Renzo Sancisi and Pirin Erdogdu for helpful discussions during the early stages of this project. Finally, we thank the anonymous referee for helpful suggestions to improve the paper.

REFERENCES

Aaronson M., Mould J., 1983, ApJ, 265, 1
Bamford S. P., Aragón-Salamanca A., Milvang-Jensen B., 2006, MNRAS, 366, 308
Bell E. F., de Jong R. S., 2001, ApJ, 550, 212
Böhm A., Ziegler B. L., 2006, ArXiv Astrophysics e-prints: astro-ph/0601505
Böhm A., Ziegler B. L., Saglia R. P., Bender R., Fricke K. J., Gabasch A., Heidt J., Mehlert D., Noll S., Seitz S., 2004, A&A, 420, 97
Bullock J. S., Kolatt T. S., Sigad Y., Somerville R. S., Kravtsov A. V., Klypin A. A., Primack J. R., Dekel A., 2001, MNRAS, 321, 559
Chiu K., Bamford S. P., Bunker A., 2007, ArXiv Astrophysics e-prints
Courteau S., 1997, AJ, 114, 2402
Courteau S., Andersen D. R., Bershady M. A., MacArthur L. A., Rix H., 2003, ApJ, 594, 208
Courteau S., Rix H., 1999, ApJ, 513, 561
Dalcanton J. J., Spergel D. N., Summers F. J., 1997, ApJ, 482, 659
de Rijcke S., Zeilinger W. W., Hau G. K. T., Prugniel P., Dejonghe H., 2007, ApJ, 659, 1172
de Vaucouleurs G., de Vaucouleurs A., Buta R., 1983, AJ, 88, 764
Flores H., Hammer F., Puech M., Amram P., Balkowski C., 2006, A&A, 455, 107
Franx M., de Zeeuw T., 1992, ApJ, 392, L47
Geha M., Blanton M. R., Masjedi M., West A. A., 2006, ApJ, 653, 240
Gerhard O., Kronawitter A., Saglia R. P., Bender R., 2001, AJ, 121, 1936
Giovanelli R., Haynes M. P., Herter T., Vogt N. P., da Costa L. N., Freudling W., Salzer J. J., Wegner G., 1997, AJ, 113, 53
Giovanelli R., Haynes M. P., Salzer J. J., Wegner G., da Costa L. N., Freudling W., 1994, AJ, 107, 2036
Giovanelli R., Haynes M. P., Salzer J. J., Wegner G., da Costa L. N., Freudling W., 1995, AJ, 110, 1059
Haynes M. P., Giovanelli R., 1984, AJ, 89, 758
Hinz J. L., Rix H., Bernstein G. M., 2001, AJ, 121, 683
Mathieu A., Merrifield M. R., Kuijken K., 2002, MNRAS, 330, 251
McGaugh S. S., 2005, ApJ, 632, 859
McGaugh S. S., Schombert J. M., Bothun G. D., de Blok W. J. G., 2000, ApJ, 533, L99
Milvang-Jensen B., Aragón-Salamanca A., Hau G. K. T., Jørgensen I., Hjorth J., 2003, MNRAS, 339, L1
Navarro J. F., Steinmetz M., 2000, ApJ, 538, 477
Noordermeer E., van der Hulst J. M., 2007, MNRAS, 367, 1480
Noordermeer E., van der Hulst J. M., Sancisi R., Swaters R. A., van Albada T. S., 2005, A&A, 442, 137
Noordermeer E., van der Hulst J. M., Sancisi R., Swaters R. A., van Albada T. S., 2007, MNRAS, 367, 1513 (N07)
Palunas P., Williams T. B., 2000, AJ, 120, 2884
Peletier R. F., Willner S. P., 1993, ApJ, 418, 626
Pizagno J., Prada F., Weinberg D. H., Rix H.-W., Pogge R. W., Grebel E. K., Harbeck D., Blanton M., Brinkmann J., Gunn J. E., 2006, ArXiv Astrophysics e-prints: astro-ph/0608472
Portinari L., Sommer-Larsen J., 2007, MNRAS, 375, 913
Rix H.-W., Guhathakurta P., Colless M., Ing K., 1997, MNRAS, 285, 779
Roberts M. S., 1978, AJ, 83, 1026
Rubin V. C., Burstein D., Ford W. K., Thonnard N., 1985, ApJ, 289, 81
Russell D. G., 2004, ApJ, 607, 241
Schlegel D. J., Finkbeiner D. P., Davis M., 1998, ApJ, 500, 525
Simard L., Pritchet C. J., 1998, ApJ, 505, 96
Spekkens K., Giovanelli R., 2006, AJ, 132, 1426 (S06)
Sprayberry D., Bernstein G. M., Impey C. D., Bothun G. D., 1995, ApJ, 438, 72
Swaters R. A., van Albada T. S., van der Hulst J. M., Sancisi R., 2002, A&A, 390, 829
Tully R. B., Fisher J. R., 1977, A&A, 54, 661
Tully R. B., Fouqué P., 1985, ApJS, 58, 67
Tully R. B., Mould J. R., Aaronson M., 1982, ApJ, 257, 527
Tully R. B., Pierce M. J., 2000, ApJ, 533, 744
Tully R. B., Pierce M. J., Huang J., Saunders W., Verheijen M. A. W., Witchalls P. L., 1998, AJ, 115, 2264
Tully R. B., Verheijen M. A. W., Pierce M. J., Huang J., Wainscoat R. J., 1996, AJ, 112, 2471 (T96)
Verheijen M. A. W., 1997, PhD thesis, Rijksuniversiteit Groningen
Verheijen M. A. W., 2001, ApJ, 563, 694 (V01)
Verheijen M. A. W., Sancisi R., 2001, A&A, 370, 765
Visvanathan N., 1981, A&A, 100, L20
Vogt N. P., Forbes D. A., Phillips A. C., Gronwall C., Faber S. M., Illingworth G. D., Koo D. C., 1996, ApJ, 465, L15
Vogt N. P., Phillips A. C., Faber S. M., Gallego J., Gronwall C., Guzman R., Illingworth G. D., Koo D. C., Lowenthal

J. D., 1997, ApJ, 479, L121
Weiner B. J., Willmer C. N. A., Faber S. M., Harker J., Kassin S. A., Phillips A. C., Melbourne J., Metevier A. J., Vogt N. P., Koo D. C., 2006, ApJ, 653, 1049
Willick J. A., 1999, ApJ, 516, 47
Ziegler B. L., Böhm A., Fricke K. J., Jäger K., Nicklas H., Bender R., Drory N., Gabasch A., Saglia R. P., Seitz S., Heidt J., Mehlert D., Möllenhoff C., Noll S., Sutorius E., 2002, ApJ, 564, L69
Zwaan M. A., van der Hulst J. M., de Blok W. J. G., McGaugh S. S., 1995, MNRAS, 273, L35